

July 7, 2014

Azimuthal Emission Patterns of K^+ and of K^- Mesons in Ni + Ni Collisions near the Strangeness Production Threshold

V. Zinyuk,^{1,*} T.I. Kang,^{2,3,†} Y. Leifels,² N. Herrmann,¹ B. Hong,³ R. Averbeck,² A. Andronic,² V. Barret,⁴ Z. Basrak,⁵ N. Bastid,⁴ M.L. Benabderrahmane,¹ M. Berger,^{6,7} P. Buehler,⁸ M. Cargnelli,⁸ R. Čaplar,⁵ I. Carevic,⁹ P. Crochet,⁴ I. Deppner,¹ P. Dupieux,⁴ M. Dželalija,⁹ L. Fabbietti,^{6,7} Z. Fodor,¹⁰ P. Gasik,¹¹ I. Gašparić,⁵ Y. Grishkin,¹² O.N. Hartmann,² K.D. Hildenbrand,² J. Kecskesteti,¹⁰ Y.J. Kim,² M. Kirejczyk,¹¹ M. Kiš,^{2,5} P. Koczon,² R. Kotte,¹³ A. Lebedev,¹² A. Le Fèvre,² J.L. Liu,^{1,14} X. Lopez,⁴ V. Manko,¹⁵ J. Marton,⁸ T. Matulewicz,¹¹ R. Münzer,^{6,7} M. Petrovici,¹⁶ K. Piasecki,¹¹ F. Rami,¹⁷ A. Reischl,¹ W. Reisdorf,² M.S. Ryu,³ P. Schmidt,⁸ A. Schüttauf,² Z. Seres,¹⁰ B. Sikora,¹¹ K.S. Sim,³ V. Simion,¹⁶ K. Siwek-Wilczyńska,¹¹ V. Smolyankin,¹² K. Suzuki,⁸ Z. Tyminski,¹¹ P. Wagner,¹⁷ E. Widmann,⁸ K. Wiśniewski,^{1,11} Z.G. Xiao,¹⁸ I. Yushmanov,¹⁵ Y. Zhang,^{1,19} A. Zhilin,¹² and J. Zmeskal⁸

(FOPI Collaboration)

E. Bratkovskaya^{20,21} and C. Hartnack²²

¹Physikalisches Institut der Universität Heidelberg, Heidelberg, Germany

²GSI Helmholtzzentrum für Schwerionenforschung GmbH, Darmstadt, Germany

³Korea University, Seoul, Korea

⁴Laboratoire de Physique Corpusculaire, IN2P3/CNRS, and Université Blaise Pascal, Clermont-Ferrand, France

⁵Ruder Bošković Institute, Zagreb, Croatia

⁶Excellence Cluster Universe, Technische Universität München, Garching, Germany

⁷E12, Physik Department, Technische Universität München, Garching, Germany

⁸Stefan-Meyer-Institut für subatomare Physik, Österreichische Akademie der Wissenschaften, Wien, Austria

⁹University of Split, Split, Croatia

¹⁰Wigner RCP, RMKI, Budapest, Hungary

¹¹Institute of Experimental Physics, Faculty of Physics, University of Warsaw, Warsaw, Poland

¹²Institute for Theoretical and Experimental Physics, Moscow, Russia

¹³Institut für Strahlenphysik, Helmholtz-Zentrum Dresden-Rossendorf, Dresden, Germany

¹⁴Harbin Institute of Technology, Harbin, China

¹⁵Kurchatov Institute, Moscow, Russia

¹⁶Institute for Nuclear Physics and Engineering, Bucharest, Romania

¹⁷Institut Pluridisciplinaire Hubert Curien and Université de Strasbourg, Strasbourg, France

¹⁸Department of Physics, Tsinghua University, Beijing 100084, China

¹⁹Institute of Modern Physics, Chinese Academy of Sciences, Lanzhou, China

²⁰Frankfurt Institute for Advanced Studies, Frankfurt am Main, Germany

²¹Institute for Theoretical Physics, Johann Wolfgang Goethe Universität, Frankfurt am Main, Germany

²²SUBATECH, UMR 6457, Ecole des Mines de Nantes - IN2P3/CNRS - Université de Nantes, Nantes, France

Azimuthal emission patterns of K^\pm mesons have been measured in Ni + Ni collisions with the FOPI spectrometer at a beam kinetic energy of 1.91 A GeV. The transverse momentum p_T integrated directed and elliptic flow of K^+ and K^- mesons as well as the centrality dependence of p_T -differential directed flow of K^+ mesons are compared to the predictions of HSD and IQMD transport models. The data exhibits different propagation patterns of K^+ and K^- mesons in the compressed and heated nuclear medium and favor the existence of a kaon-nucleon in-medium potential, repulsive for K^+ mesons and attractive for K^- mesons.

PACS numbers: 25.75.-q; 25.75.Dw; 25.75.Ld

I. INTRODUCTION

Relativistic heavy-ion collisions at bombarding energies of 1-2 A GeV provide the unique possibility to study

nuclear matter at high temperatures, around 100 MeV, and baryon densities about 2-3 times the normal nuclear matter density(ρ_0) [1, 2]. Under these conditions, the properties of hadrons may be altered as a result of various non-trivial in-medium effects like the partial restoration of the spontaneously broken chiral symmetry, the modified baryon-meson couplings, and the nuclear potential. Whether and how hadronic properties, such as masses, widths and dispersion relations are mod-

*Electronic address: v.zinyuk@gsi.de

†Electronic address: t.i.kang@gsi.de

ified in the hot and dense nuclear medium is a topic of great current interest. In particular, strange mesons produced around the production threshold energies in nucleon-nucleon collisions are considered to be sensitive to in-medium modifications. Various theoretical approaches agree qualitatively predicting slightly repulsive KN - and strongly attractive $\bar{K}N$ potentials [3]. The depth of the $\bar{K}N$ potential at finite densities is, however, not well constrained by currently available data and is a matter of an active theoretical dispute [4]. If the K^-N potential is sufficiently deep, this might have exciting consequences for the stability of neutron stars [5] or for the existence of deeply bound K^- states [6].

Heavy-ion experiments, with the capability to identify kaons and antikaons, have been performed with the KaoS, FOPI and HADES detector systems at the heavy-ion synchrotron (SIS) of GSI, aiming at measuring the in-medium properties. A significantly enhanced yield of K^- mesons relative to that of K^+ [7, 8], an increase of the K^-/K^+ ratio at low kinetic energy of kaons [8, 9], and different freeze-out conditions of K^+ and K^- mesons were observed [10], the latter at least partially explained by the production of ϕ mesons [11]. After the suggestion that the KN potential should manifest itself in the collective motion of kaons, referred to as ‘flow’ [12], a lot of effort was invested to deduce the strength of the kaon potential by measuring the kaon flow in heavy-ion collisions [13–16]. Experimental difficulties due to the small production rate of K^- mesons in comparison to K^+ in the SIS energy regime restrict the measurements. Currently available flow results for K^- mesons are not sufficient to draw conclusions on the existence and strength of the $\bar{K}N$ in-medium potential.

In this article, we report for the first time on the simultaneous measurements of K^+ and K^- mesons with a large acceptance spectrometer at an incident beam energy of 1.91 AGeV that is close to the various strangeness production threshold energies. The data are compared to state-of-the-art transport calculations with and without the assumption of an in-medium potential. In particular, we show the azimuthal anisotropy of K^- mesons in a wide range of rapidity and the centrality dependence of p_T differential flow of K^+ mesons.

II. DATA ACCUMULATION AND ANALYSIS

The experiment was performed with the FOPI spectrometer, an azimuthally symmetric apparatus comprising several sub detectors [17]. Recently a high resolution highly granular time-of-flight (ToF) Barrel based on Multi-strip Multi-gap Resistive Plate Counters (MMRPC) [18] was added to the FOPI apparatus improving significantly the kaon identification capability. Charged kaons are identified based on the ToF-information from MMRPC and Plastic Scintillator Barrel (PSB), combined with the momentum information from the Central Drift Chamber (CDC, $27^\circ < \theta_{lab} < 113^\circ$), see Table I.

TABLE I: Charged kaon acceptance in terms of laboratory momentum and polar angle are shown with corresponding signal-to-background-ratios (S/B) (see text for details).

ToF	θ_{lab} (deg)	K^+		K^-	
		p_{lab} (GeV/c)	S/B	p_{lab} (GeV/c)	S/B
MMRPC	[30, 55]	[0.13, 0.9]	> 22	[0.13, 0.7]	> 8
PSB	[55, 110]	[0.13, 0.55]	> 10	[0.13, 0.45]	> 4

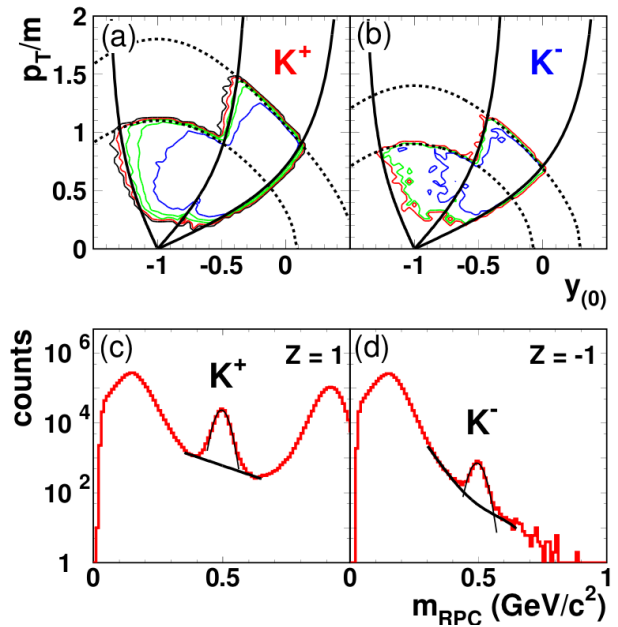


FIG. 1: (color online) Upper panel: Measured yield of K^+ and K^- mesons: p_T/m_K as a function of $y_{(0)}$. The contour levels correspond to logarithmically increasing intensity. The solid curves denote the geometrical limits of the detector acceptance ($\theta_{lab} = 30^\circ, 55^\circ$ and 110°). The dashed curves corresponds to $p_{lab} = 0.55$ and 0.9 GeV/c for K^+ (left) and $p_{lab} = 0.45$ and 0.7 GeV/c for K^- (right). Lower panel: The mass spectra from MMRPC for $Z = 1$ and -1 . The solid lines represent Gaussian fit functions for the signal and exponential functions for the background (see text for details).

The acceptance range of the detector for K^\pm is shown in the upper panel of Fig. 1 in terms of normalized transverse momentum, p_T/m , and normalized rapidity, $y_{(0)} = y_{lab}/y_{cm} - 1$, defined to be +1 (-1) at projectile (target) rapidity. About 69×10^6 events were recorded, triggering on the most central 60% of the total geometrical cross section ($\sigma_{trig} = 1.6$ b). In total, 233,300 K^+ and 5,200 K^- mesons were identified within 2σ around the fitted signal peaks from ToF mass spectra (as visualized for the MMRPC in Fig. 1, lower panel). In order to account for the contamination from pions and protons as well as misidentified tracks the background distribution was estimated in a worst-case scenario, i.e. as linear background connecting the minima around the fitted signal peaks in the mass spectra. Following these definitions for

‘signal’ and ‘background’ the signal-to-background-ratios (S/B), as listed in Table I, were estimated. The events were sorted into different centrality intervals by imposing conditions on the baryon multiplicity (Mul), shown in Table II. The baryon multiplicity contains all charged particles from the Plastic Wall ($6.5^\circ < \theta_{lab} < 23^\circ$) and p, d, t, ^3He and ^4He from the CDC. The reaction plane was reconstructed event-wise by the transverse momentum method [19] including all particles except identified pions and kaons within the CDC and Plastic Wall acceptance outside the mid-rapidity interval $|y_{(0)}| < 0.3$. The particle of interest was excluded in order to avoid autocorrelations.

The phenomenon of collective flow [20] can be quantitatively described in terms of anisotropies of the azimuthal emission pattern, expressed by a Fourier series:

$$\frac{dN}{d\phi} \propto (1 + 2v_1 \cos(\phi) + 2v_2 \cos(2\phi) + \dots), \quad (1)$$

where ϕ is the azimuthal angle of the outgoing particle with respect to the reaction plane [21]. The first order Fourier coefficient, v_1 , describes the collective sideward deflection of particles in the reaction plane, called ‘directed flow’. The second order Fourier coefficient, v_2 , describes the emission pattern in- versus out- of the reaction plane, referred to as ‘elliptic flow’ [15, 22]. The Fourier coefficients are corrected for the accuracy of the reaction plane determination according to the Ollitrault method [23]. The mean correction values, f_1 and f_2 (given in Table II) are calculated separately for each evaluated centrality(multiplicity) interval. The correction values f_n are applied to the measured v_n values according to the event’s multiplicity. Possible resolution effects due to wide centrality bins, as discussed in [24], were investigated and found to be negligible for the present analysis. Note that the most peripheral events ($\text{Mul} < 20$) were rejected to assure a minimal accuracy of the reaction plane determination.

TABLE II: Definition of event classes: (a) total, (p) peripheral and (c) central events. The corresponding cross section σ , mean impact parameter $\langle b \rangle$, the r.m.s. of b distribution: Δb and the reaction plane correction factors f_1 for v_1 and f_2 for v_2 are listed.

	Mul	σ (b)	$\langle b \rangle \pm \Delta b$ (fm)	f_1	f_2
(a)	[20, 90]	1.09 ± 0.10	3.90 ± 1.41	1.5 ± 0.1	3.0 ± 0.1
(p)	[20, 48]	0.79 ± 0.05	4.54 ± 0.95	1.5 ± 0.1	3.0 ± 0.1
(c)	[49, 90]	0.30 ± 0.05	2.11 ± 0.80	1.6 ± 0.1	3.1 ± 0.2

III. RESULTS

The experimental data on v_1 and v_2 of K^\pm for the total event sample (a) (see Table II) are presented as

function of $y_{(0)}$ in Fig. 2 and Fig. 3. v_1 is by definition antisymmetric with respect to mid-rapidity, therefore it should vanish at mid-rapidity for a symmetric collision system. However, we observe, like in other FOPI data [15][25], a deviation from zero. Systematic investigation of v_1 at mid-rapidity ($y_0 = 0$) showed a dependence on centrality, particle type and system size suggesting a correlation with track density. When reconstructing the reaction plane with the best possible accuracy (i.e. largest polar angle range $6.5^\circ < \theta_{lab} < 113^\circ$) the v_1 at mid-rapidity was found to be independent of transverse momentum in the system Ni+Ni at 2A GeV. The origin of the v_1 -‘shift’ was investigated by means of Monte Carlo study using the GEANT3 package [26]. Within the Monte Carlo framework the FOPI apparatus is described including the resolution in energy deposition and spatial position, front-end electronic processing, hit reconstruction, hit tracking and track matching between the sub-detectors. The output of GEANT was analyzed in the same way as the experimental data. As observed in the data, the v_1 -‘shift’ at mid-rapidity was found to depend on centrality and particle type, and to be independent of transverse momentum. However, the magnitude of the shift is underestimated by the simulation, and hence the Monte Carlo data can not be used to correct the experimental values quantitatively. We adopt a conservative approach and attribute the full shift at mid-rapidity as systematic uncertainty (boxes in Fig. 2 and Fig. 4). Since the local track density seen by the CDC only depends on the azimuthal angle and not on the polar angle we assume the systematic uncertainty to be rapidity independent.

The v_1 values of K^- are compatible with zero within the statistical sensitivity of the data (Fig. 2) In order to reduce the statistical error, Fig. 2 also contains a K^- data point with an upper momentum limit of 1.0 GeV/c (star symbol) from subset of runs with improved resolution.

Near target rapidity K^+ mesons show a collective in-plane deflection in the direction opposed to that of protons (Fig. 2). This pattern is called ‘anti-flow’ and is in agreement with previous FOPI measurement [15]. Additionally the K^+ mesons are observed to collectively move out-of-plane (Fig. 3) as indicated by the negative v_2 values. In case of K^- mesons (Fig. 2 (c) and Fig. 3 (c)), both v_1 and v_2 are compatible with zero within the statistical sensitivity of the data, i.e. an isotropic emission pattern is observed.

The KaoS collaboration has measured v_2 coefficients of K^\pm to be $v_2(K^+) = -0.05 \pm 0.03$ and $v_2(K^-) = -0.09 \pm 0.06$ at mid-rapidity for the same collision system at the same beam energy, however, with a different detector acceptance and collision centrality ($3.8 < b_{geo} < 6.5$ fm) [16]. The v_2 values from our data, reduced to the same centrality range and acceptance, are compatible with the KaoS results, but do not show any indication for in-plane emission of K^- mesons.

In order to link the flow measurements to the K^\pm properties in the nuclear medium, a comparison to the

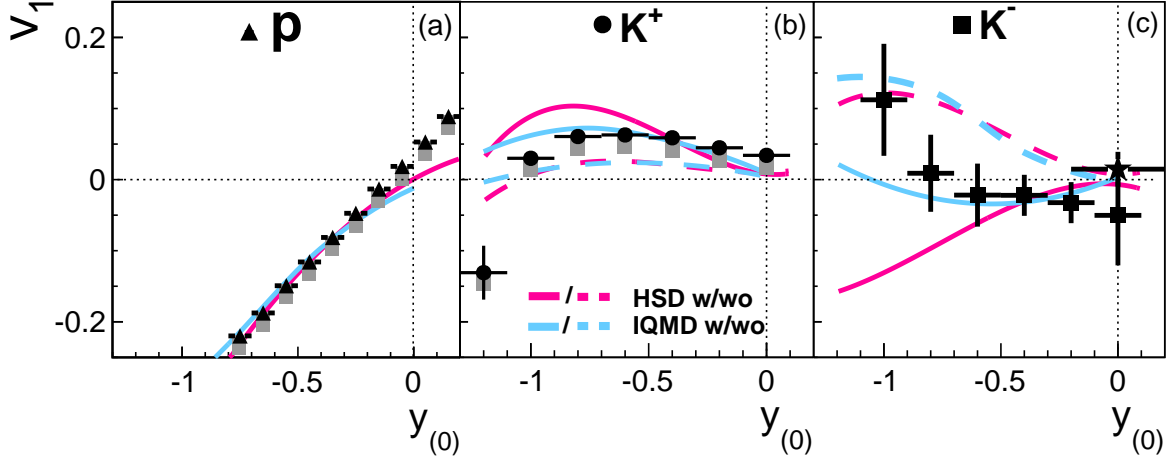


FIG. 2: (color online) Rapidity dependence of v_1 for protons (a), K^+ (b) and K^- mesons (c), in comparison to HSD and IQMD with ('w') and without ('wo') in-medium potential. Error bars (boxes) denote statistical (systematic) uncertainties. The star symbols for K^- mesons at mid-rapidity in (c) are from the high statistics data in the range $p < 1.0$ GeV/ c with $S/B > 5$.

predictions of transport model calculations is necessary. For this analysis we utilize the Hadron String Dynamics (HSD) model [27] and Isospin Quantum Molecular Dynamics (IQMD) [28] offering a state-of-the-art description of kaon dynamics [4]. The models employ different in-medium scenarios for the modification of strange particle properties in the dense and hot medium: in HSD the chiral perturbation theory [29] for kaons and a coupled channel G-matrix approach [30] for antikaons are implemented. In IQMD transport approach the relativistic mean-field model for kaons and antikaons based on a chiral SU(3) model is used [31].

The centrality selection imposed on the data is realized by weighting the events with an impact parameter dependent function. This function is obtained by evaluating the influence of a multiplicity selection on the impact parameter distribution within the IQMD model which describes the multiplicity distribution – after cluster formation – reasonably well. Earlier data on flow of K^+ mesons [15] and the K_s^0 spectra in pion induced reactions [32] were successfully described by HSD with a repulsive KN potential of 20 ± 5 MeV for particles at rest ($p = 0$), at normal nuclear matter density and a linear dependence on baryon density. Employing this parametrization for the K^+N potential in both HSD and IQMD, and a similar, but attractive one with $U_{K^-N}(\rho = \rho_0, p = 0) = -45$ MeV in IQMD and a G-Matrix formalism corresponding to $U_{K^-N}(\rho = \rho_0, p = 0) = -50$ MeV in HSD for the K^-N potential the model predictions depicted by the full lines in Fig. 2 and Fig. 3 are obtained. The phase space distributions obtained from the transport calculations are filtered for the detector acceptance. The flow observables are calculated using the true reaction plane. Typical statistical uncertainties in the calculations are of

the order $\Delta v_1 \approx 0.005$ and $\Delta v_2 \approx 0.01$. The effect of the in-medium potentials is visible in the difference to the model calculations without in-medium potential (dashed lines) that still include $K^\pm N$ rescattering and absorption processes for K^- mesons.

Inspection of Fig. 2 reveals that according to the transport models the largest sensitivity to the presence of in-medium potentials is achieved with the sideflow observable, v_1 , near target rapidity. Without any in-medium modifications the K^+ mesons should be emitted nearly isotropic, i.e. v_1 and v_2 values are close to zero. The presence of a repulsive K^+N potential manifests itself by pushing the K^+ mesons away from the protons, thus generating the 'anti-flow' signature of K^+ mesons. The magnitude of the 'anti-flow' is correctly described by IQMD transport approach with the assumption of a K^+N potential of 20 ± 5 MeV, while HSD predicts the 'anti-flow' effect but quantitatively overestimates the magnitude of the experimentally observed 'anti-flow'. For K^- mesons the interpretation is different: because of the strong absorption due to strangeness exchange reactions with baryons, an 'anti-flow' signature is expected without the presence of a potential (Fig. 2). This is clearly disfavored by the data. Assuming an additional attraction of K^- toward protons, due to strong interaction, the IQMD transport model predicts an almost isotropic emission pattern, as it is observed in the data. HSD predicts a strong 'flow' signature in the near target region, though. Following both model predictions the data indicate the presence of an attractive K^-N potential. Following the IQMD approach, the depth of the potential can be constrained to $U_{K^-N}(\rho = \rho_0, p = 0) = -40 \pm 10$ MeV.

The second harmonic v_2 of K^+ mesons (Fig. 3) shows a squeeze-out signature at mid-rapidity that is explained

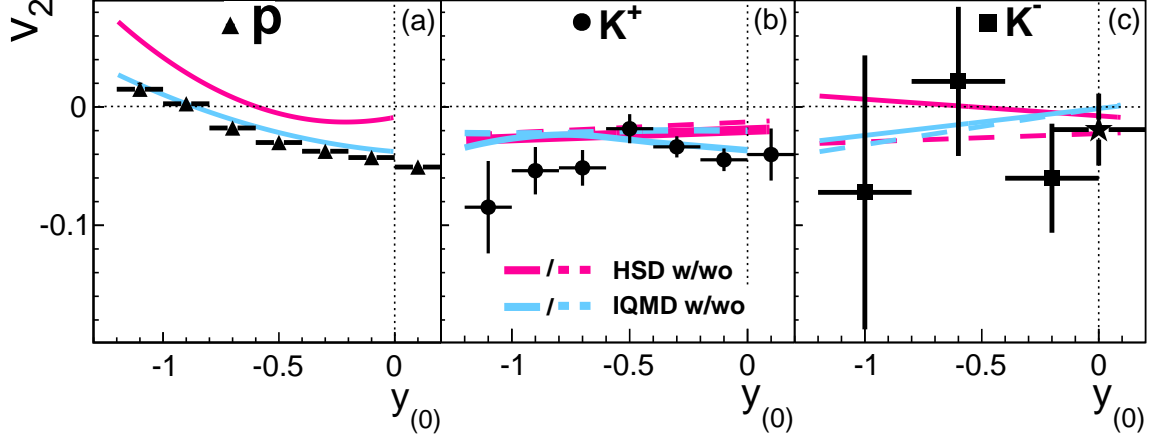


FIG. 3: (color online) Rapidity dependence of v_2 for protons (a), K^+ (b) and K^- mesons (c), in comparison to HSD and IQMD transport model predictions. Lines and symbols as in Fig. 2.

within the IQMD model by the presence of an in-medium potential. The HSD model predicts a weak squeeze-out effect, deviating by about $2 \Delta v_2$ from the data. Within the statistical sensitivity of the data this observable does not show any sensitivity to the potential away from mid-rapidity.

In the near target rapidity region the experimental v_2 is underestimated by both model calculations. However, the deviation is at the limit of the statistical significance. Note that also the v_2 values of protons (Fig. 3) are not reproduced by HSD. In the case of K^- elliptic flow, experimental uncertainties are too large to draw any conclusion about the K^-N potential.

To probe the consistency of the transport model description of the current data, shown in Fig. 2, we present in Fig. 4 the differential dependence of v_1 on the transverse momentum p_T for K^+ mesons near target rapidity ($-1.3 < y_{(0)} < -0.5$) for the two centrality classes (p) and (c) defined in Table II.

In the central event sample the data are compatible with both, HSD and IQMD, calculations employing the in-medium potential described above, in agreement to previously published FOPI results [15]. The IQMD calculations reproduce the transverse momentum dependence and the strength of the v_1 coefficient for low transverse momenta ($p_T < 0.4$ GeV/c). This quality of IQMD is also observed for the peripheral event sample, where the data show a slightly stronger p_T dependence as compared to the central case. Within HSD the transverse momentum dependence is strongly over-predicted leading to very large asymmetries at small p_T that are excluded by the data.

The influence of the Coulomb interaction was studied within the HSD transport model by comparing the flow patterns of K_S^0 and K^+ mesons. Both members of the isospin doublet show a similar p_T dependence of v_1 , but

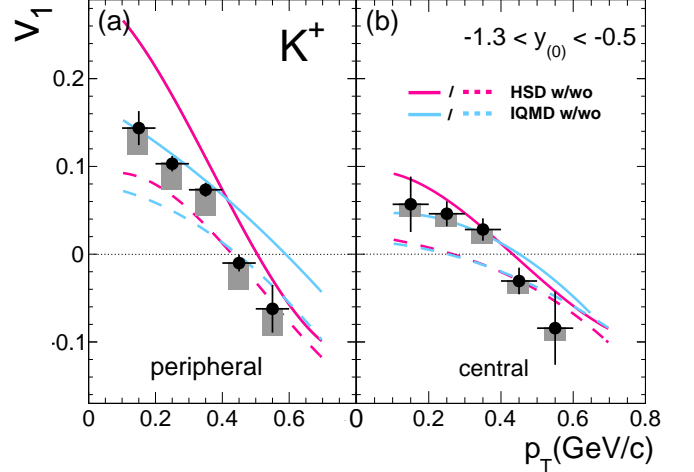


FIG. 4: (color online) Transverse momentum(p_T) dependence of v_1 distributions for K^+ mesons in peripheral (a) and central (b) collisions in comparison to HSD and IQMD predictions with (solid lines) and without (dashed lines) in-medium potentials.

in case of K^+ mesons the predicted ‘anti-flow’ is up to 12 % higher at low transverse momenta. This difference is attributed to the additional repulsion due to electromagnetic interaction between K^+ mesons and protons in the near target region. The long range influence of the Coulomb attraction/repulsion between kaons and nucleons of the projectile and target remnants was investigated with the SACA clusterization algorithm [33] which simulates the propagation of particles in the Coulomb field up to flight times of $\sim 10,000$ fm/c. Statistically significant influence was found only for the very small momenta, beneath the detector acceptance. We conclude that most of the asymmetry is caused by the strong interaction and

that v_1 can constrain the depth of the KN potential.

IV. CONCLUSIONS

We have measured the azimuthal emission patterns of K^\pm mesons in heavy-ion collisions near the strangeness production threshold energies. In case of K^+ mesons a weak in-plane ‘anti-flow’ with respect to protons and a slight ‘squeeze-out’ are observed. For K^- mesons, within large statistic uncertainties, isotropic emission pattern is observed. Despite the large uncertainties, the comparison to two independent predictions of HSD and IQMD without potential especially of the first Fourier coefficient implies the existence of a weakly attractive K^-N in-medium potential. Furthermore, the IQMD transport approach, which is able to reproduce the dynamics of nucleons and K^+ mesons, suggests a K^-N in-medium potential of $U_{K^-N} = -40 \pm 10$ MeV.

The theoretical modeling of the in-medium potentials, or more generally of the in-medium interactions, is reasonably well achieved within the IQMD transport approach as is demonstrated by the detailed comparison of the differential flow pattern of the K^+ mesons. Within

HSD, the general dynamics of nucleons and K^+ mesons is reproduced as well, however the quantitative description of the flow pattern in some regions of the phase space is not accurately achieved yet. The observed dependencies and sensitivities point to the feasibility to extract the strength of the in-medium potentials from a quantitative description of a complete set of flow data. More systematic data and theoretical efforts are clearly necessary to reach this important goal.

Acknowledgments

This work was supported by BMBF-05P12VHFC7, the KOSEF(F01-2006-000-10035-0), by BMBF-05P12RFFCQ, by the Polish Ministry of Science and Higher Education(DFG/34/2007), the agreement between GSI and IN2P3/CEA, the HIC for FAIR, the Hungarian OTKA (71989), by NSFC (project 11079025), by DAAD (PPP D/03/44611), by DFG (Projekt 446-KOR-113/76/04) and by the EU, 7th Framework Program, Integrated Infrastructure: Strongly Interacting Matter (Hadron Physics), Contract No. RII3-CT-2004-506078.

-
- [1] C. Fuchs, Prog. Part. Nucl. Phys. **56**, 1 (2006).
 - [2] B. Hong *et al.*, Phys. Rev. C **57**, 244 (1998).
 - [3] D.B. Kaplan and A.E. Nelson, Phys. Lett. B **175**, 57 (1986); G.E. Brown and M. Rho, Phys. Rev. Lett. **66**, (1991) 2720; G.Q. Li and C.M. Ko, Phys. Lett. B **338**, (1994) 118; M. Lutz, Phys. Lett. B **426**, 12 (1998); Nucl. Phys. A **574**, 755 (1994); T. Waas, N. Kaiser and W. Weise, Phys. Lett. B **379**, 34 (1996); **365**, 12 (1996).
 - [4] C. Hartnack *et al.*, Phys. Rep. **510**, 119 (2012) and references therein.
 - [5] J. Lattimer and M. Prakash, Phys. Reports **442** (2007) 109; W. Weise Prog. Part. Nucl. Phys. **67** (2012) 299.
 - [6] Y. Akaishi, T. Yamazaki, Phys. Rev. C **65**, 04405 (2002).
 - [7] D. Best *et al.*, Nucl. Phys. A **625**, 307 (1997).
 - [8] F. Laue *et al.*, Phys. Rev. Lett. **82**, 1640 (1999).
 - [9] K. Wisniewski *et al.*, Eur. Phys. J. A **9**, 515 (2000).
 - [10] A. Förster *et al.*, Phys. Rev. C **75**, 024906 (2007).
 - [11] M. Lorenz *et al.*, PoS BORMIO **2010** (2010) 038.
 - [12] G.Q. Li *et al.*, Phys. Rev. Lett. **74**, 2 (1995).
 - [13] J. Ritman *et al.*, Z. Phys. A **352**, 355 (1995).
 - [14] Y. Shin *et al.*, Phys. Rev. Lett. **81**, 1576 (1998).
 - [15] P. Crochet *et al.*, Phys. Lett. B **486**, 6 (2000).
 - [16] F. Uhlig *et al.*, Phys. Rev. Lett. **95**, 012301 (2005).
 - [17] A. Gobbi *et al.*, Nucl. Instr. Meth. A **324**, 156 (1993); J. Ritman *et al.*, Nucl. Phys. B, Proc., Suppl. **44**, 708 (1995).
 - [18] M. Kiš *et al.*, Nucl. Instr. and Meth. A **646**, 27 (2011).
 - [19] P. Danielewicz and G. Odyniec, Phys. Lett. B **157**, 146 (1985).
 - [20] N. Herrmann *et al.*, Ann. Rev. Nucl. Part. Sci. **49**, 581 (1999); W. Reisdorf and H.G. Ritter *et al.*, Ann. Rev. Nucl. Part. Sci. **47**, 663 (1997).
 - [21] S. Voloshin and Y. Zhang, Z. Phys. C **70**, 665 (1996).
 - [22] A. Andronic *et al.*, Phys. Lett. B **612**, 173 (2005).
 - [23] Jean-Yves Ollitrault, Nucl. Phys. A **638**, 195c (1998).
 - [24] H. Masui, A. Schah arXiv:1212.3650 [nucl-ex].
 - [25] W. Reisdorf *et al.*, Nucl. Phys. A **876**, 1 (2012).
 - [26] R. Brun *et al.*, CERN/DD/78-2, 1978
 - [27] W. Cassing *et al.*, Phys. Rep. **308**, 65 (1999).
 - [28] C. Hartnack *et al.*, Eur. Phys. J. A **1**, 151 (1998).
 - [29] A. Mishra *et al.*, Phys. Rev. C **70**, 044904 (2004).
 - [30] W. Cassing, L. Tolos *et al.*, Nucl. Phys. A **727**, 59 (2003).
 - [31] J. Schaffner-Bielich, I.N. Mishustin and J. Bondarf, Nucl. Phys. A **625**, 325 (1997).
 - [32] M.L. Benabderrahmane *et al.*, Phys. Rev. Lett. **102**, 182501 (2009).
 - [33] R.K. Puri and J. Aichelin, J. Comput. Phys. **162**, 245 (2000).